Conductive cooling in white organic light emitting diode for enhanced efficiency and life time

Priyanka Tyagi,[1,2,a)] Arunandan Kumar,[3] Lalat Indu Giri,[2] Suneet Tuli,[2] and Ritu Srivastava[1,b)]
[1]*CSIR-Network of Institute for Solar Energy (NISE), Physics of Energy Harvesting Division, CSIR-National Physical Laboratory, Dr. K. S. Krishnan Road, New Delhi 110012, India*
[2]*Center for Applied Research in Electronics, Indian Institute of Technology Delhi, New Delhi 110016, India*
[3]*Laboratoire Interdisciplinaire Carnot de Bourgogne, CNRS UMR 5209, Université de Bourgogne, 9 Avenue Alain Savary, Dijon, France*

(Received 28 September 2014; accepted 23 November 2014; published online 6 January 2015)

We demonstrate white organic light emitting diodes with enhanced efficiency (26.8 lm/W) and life time (~11 000 h) by improved heat dissipation through encapsulation composed of a metal (Cu, Mo, and Al) and mica sheet joined using thermally conducting epoxy. Finite element simulation is used to find effectiveness of these encapsulations for heat transfer. Device temperature is reduced by about 50% with the encapsulation. This, consequently, has improved efficiency and life time by about 30% and 60%, respectively, with respect to glass encapsulation. Conductive cooling of device is suggested as the possible cause for this enhancement. © *2015 AIP Publishing LLC*.
[http://dx.doi.org/10.1063/1.4903800]

White organic light emitting diodes (WOLEDs) presented their strong candidature in solid state lighting application in last few decades. It paves the way for efficient and cost effective lighting sources and offers superior performance over other competing solid state lighting technologies due to high color purity, low voltage operation, and availability of material combinations for white light production.[1,2] WOLEDs with multi-emissive layers are leading in terms of efficiency; however, these produce significant heating inside the device. Heating inside the device leads to significant rise of temperature and causes exciton dissociation and degradation. Thermal management in these devices may offer significant improvement of life time and efficiency.

The heat generation can be decreased by efficient dissipation using external heat sinks attached to device.[3–6] Several approaches have been adopted in optoelectronic devices for efficient heat dissipation such as heat sink, cooling panel, microstructure strip, two phase cooling, passive cooling, immersion cooling, and micro jet cooling.[3–10] In the context of OLEDs, few efficient approaches have been proposed which include fabrication of OLEDs on thermally conducting substrate, insertion of heat transfer fluid in encapsulation, use of thin film encapsulation, and immersing the whole OLED in a thermally conducting fluid.[11–14] These methods have several disadvantages such as using thermally conducting substrate is effective in reducing the device temperature; however, can only be employed for top-emitting OLEDs due to opaque nature of thermally conducting substrate.[11] Insertion of heat transfer fluid in encapsulation by Ham *et al.*[12] is used to transfer the heat from device to glass encapsulation where a heat sink has been included for heat dissipation; however, this complicates the device fabrication. Zakhidov *et al.*[13] have used high thermal conductivity hydrofluoroether liquid for heat dissipation and immersed OLED in this liquid which provided convective cooling of the device and device temperature is reduced by 8%. This approach affects the compactness of device and complicates to implement on large area devices. Thick cathode layer as heat sink has been used for bottom emitting OLEDs and found effective in improving the lifetime;[14] however, thick cathode has low resistance to stress and cracks can be formed.

A rather simplistic approach may be to use thermally conducting encapsulation keeping electrical insulation from cathode in bottom emitting OLEDs. In this work, we have designed and developed metal encapsulations to improve the heat dissipation from WOLEDs and monitored their effectiveness in improving the performance.

Encapsulations are prepared by joining electrically insulating mica sheet with metal sheet using a thermally conducting epoxy (silver). Mica provides the electrical insulation to device from metal and also has high value of heat capacity (0.88 J/gK) and temperature sustainability (700–800 °C).[15] The selected thickness of mica was 100 μm for the efficient transfer of temperature from the device to the metal sheet. Three encapsulations were prepared with different metals Al, Cu, and Mo to study the dependence of thermal conductivity. These encapsulations were termed as ENC-A, ENC-B, and ENC-C for Al, Cu, and Mo, respectively. The thickness of metal sheet and the total thickness of encapsulation were 500 and 800 μm, respectively.

WOLEDs were fabricated on indium tin oxide (ITO) coated glass substrates having a sheet resistance of 20 Ω/sq. The device structure was ITO (120 nm)/0.4 wt. % F_4-TCNQ doped α-NPD (35 nm)/5 wt. % BCzVBi doped CBP (20 nm)/5 wt. % $Ir(ppy)_3$ doped CBP (4 nm)/0.75 wt. % $Ir(btp)_2acac$ doped CBP (12.5 nm)/BAlq (30 nm)/LiF (1 nm)/Al (150 nm). Where ITO was used as anode, 0.4 wt. % F_4-TCNQ doped α-NPD as hole transport layer, 5 wt. % BCzVBi doped CBP

a)E-mail: priyanka.tyagi.193@gmail.com
b)Author to whom correspondence should be addressed. Electronic mail: ritu@nplindia.org. Tel.: 91-11-45608596.

as blue emitter, 5 wt. % $Ir(ppy)_3$ doped CBP as green emitter, and 0.75 wt. % $Ir(btp)_2acac$ doped CBP as red emitter, BAlq as electron transport layer, LiF as electron injection layer, and Al as cathode. Current density-voltage-luminescence (J-V-L) characteristics were measured with a luminescence meter (LMT-1009) interfaced with a Kiethley 2400 programmable current voltage digital source meter. All measurements were carried out at room temperature under ambient conditions. Temperature measurements were performed by using un-cooled type IR camera VarioCAMhr with spectral range of 7.5–14 μm interfaced with computer and the thermographic images were captured using IRBIS software.

To find the effectiveness of as developed encapsulations, we have performed the simulation by using COMSOL 4.2, heat transfer module.[16] This module solves the heat conduction equation by using the finite element method.[17–19] Simulations were also performed on glass encapsulation for comparison. The base temperature for all the encapsulation was selected to be 350 K and the surrounding temperature as 300 K. Fig. 1 depicts the temperature variation across the thickness of encapsulation. The temperature inside glass encapsulation varies from 350 K to 300 K from bottom to top due to the poor thermal conductivity of glass. At the same time, all the developed encapsulations (ENC-A, B, and C) have a proper heat transfer from the bottom to top and as a result the temperature of the top of encapsulation is also 350 K. Therefore, all the developed metal encapsulations can be used for efficient heat dissipation from OLEDs.

The effectiveness of these encapsulations for heat dissipation was tested on WOLEDs having CIE coordinates (0.31, 0.29). Four devices were fabricated and encapsulated with glass cover slip of 800 μm thickness, ENC-A, ENC-B, and ENC-C and for simplicity the devices were termed as devices 1, 2, 3, and 4. First operating temperature of device was measured using thermo graphic measurements by keeping the biased WOLED at the focal point the IR Camera.

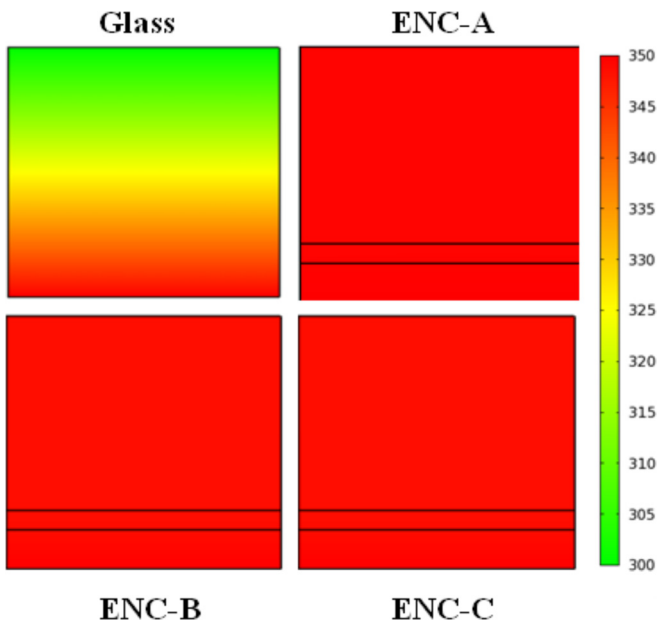

FIG. 1. Simulated temperature distribution across the glass, ENC-A, B, and C showing the efficient heat transfer in case of all developed encapsulations.

Fig. 2 depicts thermograms captured for devices 1, 2, 3, and 4. The device temperature at the center of pixel with respect to the surrounding temperature is mentioned in all the images. The device temperature is highest for device 1 with glass encapsulation and it has decreased for devices 2, 3, and 4. Device 3 with Cu encapsulation was found to possess the lowest temperature, which can be ascribed to the highest thermal conductivity of Cu among all three used metals. We have performed the measurements for 10 min, out of which, the biasing been applied for 5 min and removed for rest of the 5 min to obtain the cooling cycle.

The temperature measurements were performed at different voltages and the value of temperature rise (ΔT) with respect to room temperature for all the devices with application of voltage was obtained. Fig. 3(a) depicts the variation of ΔT of devices 1, 2, 3, and 4 with the applied voltage. The figure clearly indicates as the voltage is increased, ΔT increases for all the four devices. However, ΔT is found to decrease with metal encapsulations as compared to the glass encapsulation. The value of ΔT is 12.8 °C for device 1 with glass encapsulation at 17 V and as glass encapsulation is replaced with Al encapsulation (ENC-A) this value has reduced to 7.1 °C in device 2. This value, further, decreases to 5.7 °C and 6.3 °C with Cu (ENC-B) and Mo (ENC-C) encapsulation for devices 3 and 4. This decrease in ΔT may be attributed to the increased thermal conductivity of metal encapsulation as compared to glass. Due to this high thermal conductivity, these encapsulations provide a proper heat transfer from the device to the top of the encapsulation and can thus transfer the heat to surrounding atmosphere. The lowest value of ΔT was obtained for device 3 with Cu encapsulation because of its highest thermal conductivity (400 W/mK) value.

The cooling cycle of the device after removing the applied bias voltage is shown in Fig. 3(b) for all the devices. It is clear from the figure that devices 2, 3, and 4 attain the room temperature quickly in comparison to device 1 reflecting the proper heat dissipation through the metal encapsulation. This data then has been used to analyze the thermal

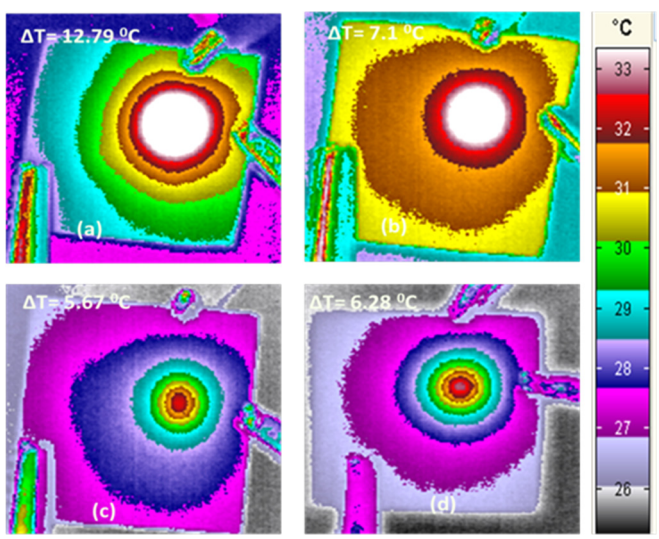

FIG. 2. Thermographic images for the devices 1, 2, 3, and 4 at 17 V.

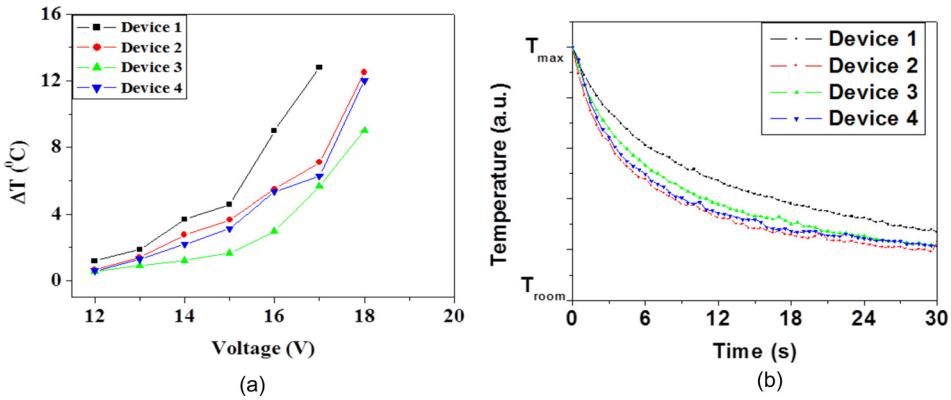

FIG. 3. (a) Variation of ΔT with voltage for device and (b) normalized variation of temperature with time at 17 V, for devices 1, 2, 3, and 4.

relaxation time. In this calculation, we have normalized the temperature at y-axis and fitted the fall part exponentially. The estimated relaxation time was found to be 6.08 s, 4.32 s, 4.45 s, and 4.00 s for devices 1, 2, 3, and 4, respectively. Therefore, thermal relaxation time has decreased for metal encapsulation in comparison to glass.

We have also measured the variation of temperature from the centre of the pixel to the edge of the substrate by taking the line profile as can be seen in Fig. 4. Figure depicts the line profile of the temperature for devices 1, 2, 3, and 4 at 17 V after 30 s. The measurements have been taken along a line as shown in the inset of this figure. This figure shows that the temperature is maximum at the center of the pixel and it decreases, symmetrically as the distance from the center increases on both directions. It is evident that the maximum of the temperature profile resides at the highest temperature for device 1 with glass encapsulation and the maximum decreases for devices 2, 3, and 4 with metal encapsulation. The lowest value of maximum temperature is observed in case of device 3 with Cu encapsulation as also observed in the previous paragraph. This measurement has been used to calculate the lateral thermal diffusion length in case of all the four devices similar to the method adopted by Chan *et al.*,[20] by fitting the temperature profile with a Gaussian distribution and the half of the width at half maximum being the diffusion length. This length is been

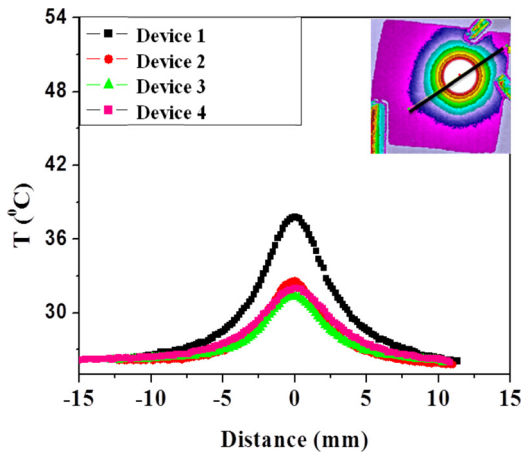

FIG. 4. Variation of temperature with distance from the center to the edge of devices 1, 2, 3, and 4 at 17 V after 30 s. The inset of the figure shows the picture of the device with the line across which the temperature variation was taken.

evaluated at different times and the lateral diffusivity was calculated using the following equation:

$$L_d = \sqrt{Dt},$$

where L_d is the diffusion length, D is the diffusivity, and t is the time. Diffusivity is obtained as the slope of square of diffusion length vs. time plot. The calculated diffusion length and diffusivity for all four devices are summarized in Table I. The calculated value of diffusion length is found to vary between 2 and 3 mm for all four devices. This diffusion length can be associated to organic layers only, because the line selected to obtain the temperature profile of device only includes the organic layers outside the device area. Therefore, the diffusion across this line has only occurred due to organic materials. The thermal diffusivity value obtained is found to be in the range of 0.029–0.09 mm^2/s. This value has ranged from 0.02 to 0.1 mm^2/s as obtained from different methods for other organic materials.[21–23] In these reports, it has been observed by Lim *et al.*,[21] Assael *et al.*,[22] and Cahill[23] that the variation observed in these measurements are the limitation of measurement techniques. Therefore, the variation in diffusivity value obtained in all four devices, in our case, may be due to the limitation of the measurement technique.

To observe the effect of the reduction of operating temperature on the device performance, luminescence was measured for all devices. Fig. 5(a) shows the variation of power efficiency (PE) with voltage for devices 1, 2, 3, and 4. The maximum value of PE is found to be 21.9 lm/W, 26.5 lm/W, 26.8 lm/W, and 26.3 lm/W for devices 1, 2, 3, and 4, respectively, at 5 V. In case of devices with metal encapsulation, the increase in PE may be attributed to the maximum harvesting of excitons because the reduction of device temperature in these devices will reduce the possibility of exciton dissociation. Excitons are generally dissociated due to higher

TABLE I. Diffusion length and the diffusivity for devices 1, 2, 3, and 4 at 17 V after 30 s.

	Diffusion length (mm)	Diffusivity (mm^2/s)
Device 1	2.46	0.085
Device 2	2.08	0.029
Device 3	2.18	0.043
Device 4	2.67	0.081

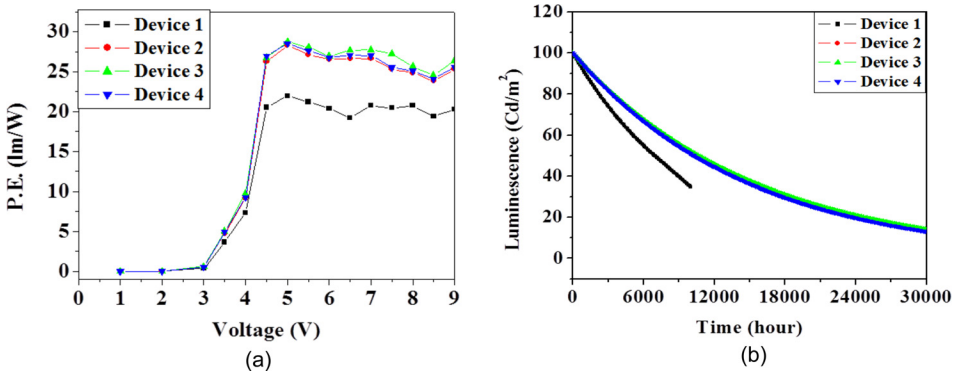

FIG. 5. (a) Variation of PE with voltage for devices 1, 2, 3, and 4. (b) Luminescence as a function of operating time showing the improvement of life time in case of WOLEDs with developed encapsulations.

operating temperature of OLEDs.[24,25] The geminate pair dissociation rate is dependent on temperature as[26]

$$k_d(T) = a \times T^{3/2} \times \exp\left(-\frac{\Delta E}{kT}\right),$$

where a is temperature independent term,[26] T is the temperature, k is Boltzmann's constant, and ΔE is binding energy of geminate pair. From this equation, it is evident that the geminate pair dissociation rate is higher for higher temperature and which is responsible for lower efficiency in case of glass encapsulated device.

Further, the luminescence has been measured as a function of operational time for lifetime measurements. Fig. 5(b) depicts the luminescence as a function of operational time for devices 1, 2, 3, and 4 at an initial luminescence of 100 Cd/m^2. This figure shows that the luminescence has decreased with the operational time for all four devices. Device 1 with glass encapsulation is found to have a faster rate of decay of luminescence as compared to devices 2, 3, and 4. We have calculated the half lifetime values for these devices, which were estimated as the time at which the luminescence reduced to half of its initial value. Devices 2, 3, and 4 with metal encapsulations are found to have an improved lifetime as compared to device 1 with glass encapsulation. Device 3 with Cu encapsulation is found to be most sustainable device with a half lifetime of 11 000 h. This increase in lifetime may be attributed to the high thermal conductivity of metal as compared to glass and Cu having the highest. Device parameters for all the four devices are summarized in Table II. The lifetime values have increased by almost 1.6 times by using the developed encapsulations with metal sheets. This table also includes the values of current efficiency (CE) and PE for these devices and it can be seen that both CE and PE have increased for devices 2, 3, and 4 with metal encapsulations as compared to device 1 with glass encapsulation. The enhancement in PE was found to be nearly 30%, 31%, and 29% in devices 2, 3, and 4 with respect to device 1. This reflects the potential of the developed encapsulations.

TABLE II. Summarization of luminescence, CE, PE, and half-life of devices 1, 2, 3, and 4.

	Luminescence at 12 V	CE (Cd/A)	PE (lm/W) at 5 V	Half life (h)
Device 1	87 500	39	20.4	6700
Device 2	87 400	50.6	26.5	10 300
Device 3	96 200	51.1	26.8	11 000
Device 4	106 100	50.3	26.3	10 200

We have designed and developed metal encapsulations with three metals Al, Cu, and Mo all with high thermal conductivity. Device temperature measurements on WOLEDs have revealed that these metal encapsulations have an efficient heat transfer from the device to the top of the encapsulation for WOLEDs. The effect of metal encapsulation has also been studied on the WOLED performance and a maximum CE of 51.1 Cd/A, PE of 26.8 lm/W, and half lifetime of 11 000 h were measured in case of Cu encapsulation. Nearly, 32%, 30%, and 60% enhancement of CE, PE, and lifetime, respectively, were observed for devices 2, 3, and 4 as compared to device 1 and the conductive cooling of the device has been suggested as the possible cause for this enhancement.

The authors gratefully recognize the financial support from Council of Scientific and Industrial Research (CSIR) New Delhi, India.

[1]S. Reineke, F. Lindner, G. Schwartz, N. Seidler, K. Walzer, B. Lüssem, and K. Leo, Nature **459**, 234 (2009).
[2]Y. Sun, N. C. Giebink, H. Kanno, B. Ma, M. E. Thompson, and S. R. Forrest, Nature **440**, 908 (2006).
[3]H. Ye, M. Mihailovic, C. K. Y. Wong, H. W. van Zeijl, A. W. J. Gielen, G. Q. Zhang, and P. M. Sarro, Appl. Therm. Eng. **52**, 353 (2013).
[4]A. Fan, R. Bonner, S. Sharratt, and Y. S. Ju, in *Proceedings of the 28th Annual IEEE Semiconductor Thermal Measurement and Management Symposium (SEMI-THERM)* (IEEE, 2012), pp. 319–324.
[5]M. Arik, Y. Utturkar, and S. Weaver, in *Proceedings of the 12th IEEE Intersociety Conference on Thermal and Thermomechanical Phenomena in Electronics Systems (ITherm)* (IEEE, 2010), pp. 1–8.
[6]A. Husain, S.-M. Kim, J.-H. Kim, and K.-Y. Kim, J. Thermophys. Heat Transfer **27**, 235 (2013).
[7]P. A. Davison, "Heat sink attachment device," U.S. patent 10/336,628 (Feb. 22, 2005).
[8]D. B. Tuckerman and R. F. W. Pease, IEEE Electron Device Lett. **2**, 126 (1981).
[9]W. B. Joyce, Solid-State Electron. **18**, 321 (1975).
[10]L. Jiang, M. Wong, and Y. Zohar, J. Microelectromech. Syst. **8**, 358 (1999).
[11]S. Chung, J.-H. Lee, J. Jeong, J.-J. Kim, and Y. Hong, Appl. Phys. Lett. **94**, 253302 (2009).
[12]H. Ham, J. Park, and Y. Kim, Org. Electron. **12**, 2174 (2011).
[13]A. A. Zakhidov, S. Reineke, B. Lüssem, and K. Leo, Org. Electron. **13**, 356 (2012).
[14]S. H. Choi, T. I. Lee, H. K. Baik, H. H. Roh, O. Kwon, and D. H. Suh, Appl. Phys. Lett. **93**, 183301 (2008).
[15]See specific heat capacity of some common solids http://www.engineeringtoolbox.com/specific-heat-solids-d_154.html.

[16]See detailed information about Heat transfer module of COMSOL http://www.comsol.fr/support/releasenotes/4.2a/heat/.
[17]G. P. Nikishkov, *Programming Finite Elements in Java* (Springer, 2010).
[18]Introduction to Heat Transfer Module, Comsol release notes, May 2013.
[19]P. Vitta and A. Žukauskas, Appl. Phys. Lett. **93**, 103508 (2008).
[20]P. K. L. Chan, K. P. Pipe, Z. Mi, J. Yang, P. Bhattacharya, and D. Lüerßen, Appl. Phys. Lett. **89**, 011110 (2006).
[21]J. Lim, J. Kim, K. Yu, E. Lim, S. Lee, and G. Park, J. Korean Phys. Soc. **32**, 228 (1998).
[22]M. J. Assael, S. Botsios, K. Gialou, and I. N. Metaxa, Int. J. Thermophys. **26**, 1595 (2005).
[23]D. G. Cahill, Rev. Sci. Instrum. **61**, 802 (1990).
[24]P. E. Burrows, Z. Shen, V. Bulovic, D. M. McCarty, S. R. Forrest, J. A. Cronin, and M. E. Thompson, J. Appl. Phys. **79**, 7991 (1996).
[25]G. Wantz, L. Hirsch, N. Huby, L. Vignau, A. S. Barrière, and J. P. Parneix, J. Appl. Phys. **97**, 034505 (2005).
[26]D. West and D. J. Binks, *Physics of Photorefraction in Polymers* (CRC Press, 2004).